Study on the Effect of Shaft Bow using a Multi Mass Flexible Rotor Model

Soumendu Jana and V. Arun Kumar
Scientist, Propulsion Division, NAL, Bangalore – 560 017

Abstract
The effect of initial shaft bow on the unbalance response of a rotor bearing system has been studied using a multi mass flexible rotor model. The equations of motion of the rotor-bearing model have been derived following finite element method and solved for unbalance response in presence of initial shaft bow using Runge-Kutta routine available in MATLAB. Typical unbalance response characteristic of bent shaft, i.e. self-balancing at certain speed, has been clearly brought out through the simulation results. Response phase angle has also been obtained from the simulation results. Experiments have been conducted up to the rotor speed of 5000 rpm, which is above the first critical speed, for validation of the simulation results partly. The initial shaft bow and unbalance level as provided in the experimental rig has been incorporated in the simulation model. There is good agreement between the experimental and the simulation results.

Keywords: *Rotor, Shaft Bow, Unbalance Response, FEM, Simulation, Experiment*

1. Introduction

The shaft bow in a rotor-bearing system is one kind of rotor defects resulting mainly from thermal effects, gravity sag or shrink fits of the rotor components. Vibration characteristics of a rotor-bearing system having bowed shaft is different from vibration due to unbalance. It is important to know whether the cause of vibration is unbalance or shaft bow, particularly from balancing point of view. The effect of shaft bow on the response of a rotor-bearing system and balancing of bowed shaft has drawn attention of several researchers. Detailed analysis of rotor response with shaft bow and balancing has been presented by Nicholas et al. [1] considering a single mass flexible rotor with bowed shaft. The effects of the magnitude and phase of bow with respect to unbalance on the rotor response have been clearly brought out through theoretical and experimental results. Salmone and Gunter [2] have studied the response of a rotor with shaft bow and skewed disk. Transfer matrix method used for the response analysis. It has been concluded that the rotor response analysis considering only the unbalance would be incorrect as the shaft bow and skewed disk affect the response dominantly. More details regarding the vibration analysis and balancing can be found in [3,4,5]. In another work experimental results are reported by Parkinson et al. [6] for a long flexible shaft which demonstrates the effects of initial shaft bow at speeds up to fourth critical speed. It has been reported that the experimental result shows very small response amplitude near the first and fourth critical speed, which is the typical unbalance response characteristic of a bent shaft.

In most of the earlier work a single mass rotor model has been considered for the theoretical analysis. In the present work an attempt has been made to study the response characteristics of a multi mass flexible rotor with shaft bow using finite element technique. A rotor model with three mid-span disks spaced at equal distance on the shaft and supported on two ball bearings at the ends has been considered for this purpose. The finite element model of the rotor-bearing system has been developed employing finite beam element for the shaft. The mid-span disks are considered as rigid disk. The bow effect has been taken care by considering the bowed shape of the shaft appropriately. Attempt has been made to compare the theoretical results with that obtained from experimental rig up to a speed above the first critical speed.

2. Rotor Model

The rotor-bearing model consists of three rigid disks mounted on a shaft and the shaft is supported by two bearings at the ends. The shaft is modeled using Timoshenko beam element [7]. The finite beam element is shown in Fig. 1. Two node points are associated with each element. There are four displacement coordinates, two translations in orthogonal radial direction and two rotations about the orthogonal radial axes, associated with each nodal point. The nodal coordinates q1, q2, q3 and q4 are associated with node 1 and node 2 is associated with q5, q6, q7 and q8. Coordinates q1, q2, q5, q6 represents the translation degrees of freedom and q3, q4, q7, q8 represents the rotational degrees of freedom. L is the length of the shaft element. Translations of a point in the shaft element at a distance s

from one end are denoted by x and y along the X and Y coordinates, respectively, of the fixed reference frame XYZ. The rotations of any point are denoted by α and β as shown in Fig. 1. The displacements x, y, α, β can be expressed in terms of the eight nodal coordinate vectors through shape functions. The equations of motion for the shaft element have been derived following considering the kinetic and potential energy associated with the element for small displacements.

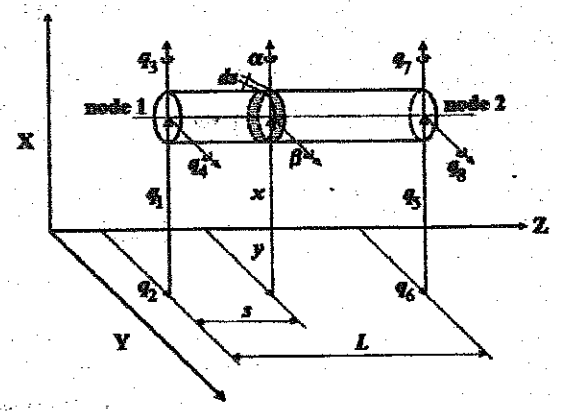

Fig. 1 The Finite Shaft Element

The disks are modeled as rigid body and disk geometric center is assumed to be coinciding with the shaft axis. Mass unbalances are assumed at the disk locations. The equations of motion of the rotor components are derived using extended Hamilton's principle. The overall systems mathematical model is formulated by assembling the component level equations of motion together. Natural boundary conditions at the bearing locations are imposed on the free-free rotor equations of motion. The assembled global equation of motion of the rotor-bearing system including the unbalance force may be written as

$$[M]\{\ddot{q}_u\}+[C]\{\dot{q}_u\}+[K]\{q_u\}=\{F(t)\}. \tag{1}$$

Where, $[M]$, $[C]$, and $[K]$ are the system mass, damping and stiffness matrices respectively. The global displacement vector is represented by $\{q_u\}$. The unbalance force vector is represented by $\{F(t)\}$.

In case of bowed shaft the displacements of the rotor nodal coordinates as observed from the fixed reference frame are the resultant of response due to unbalance force and initial bow vector. In mathematical terms the net displacement vector $\{p\}$ can be represented as [1]

$$\{p\}=\{q_o\}+\{q_u\}. \tag{2}$$

Where, $\{q_o\}$ is the initial bow vector and $\{q_u\}$ is the response due to unbalance force. Considering equation (1) and (2) the equations of motion of a rotor-bearing system with initial shaft bow may be written as

$$[M]\{\ddot{p}\}+[C]\{\dot{p}\}+[K]\{p-q_o\}=\{F(t)\}. \tag{3}$$

Equation (3) may be rewritten as,

$$[M]\{\ddot{p}\}+[C]\{\dot{p}\}+[K]\{p\}=[K]\{q_o\}+\{F(t)\}. \tag{4}$$

Equation (4) has been solved for the unbalance response using Runge-Kutta routine.

2.1 Shaft Bow Vector

It has been mentioned earlier that the shaft in a rotor-bearing system may bend mainly due to thermal effect, gravity sagging or shrink fit of mechanical components. In the present analysis it is assumed that the bending of the shaft is due to shrink fit. In this case compressive load acts along the shaft axis, which may cause the shaft to bend. The

known level of bow in the experimental rig has been created in a similar manner by tightening the end nuts on the shaft. The shape of the bow can be approximated [8] by the following expression.

$$u = ASin\left(\frac{\pi w}{L_t}\right). \tag{5}$$

Where, u is the magnitude of bow at a distance w along the shaft, L_t is the total shaft length and A is a constant, which depends on shaft end conditions. The magnitudes of bow at all the node points along the shaft axis have been calculated using equation (5). These values of the shaft bow have been incorporated in equation (4) to take care of the bow effect.

3. Simulation

The unbalance response of the rotor-bearing model has been obtained by solving equation (4) incorporating the bow effect. The system matrices are computed following finite element method and the bow magnitudes are calculated using equation (5). The magnitude of shaft bow assumed at the middle disk is approximately 200 micron, which is in accordance with the measured bow from the experimental rig. The shaft length is taken as 300 mm and the shaft diameter is taken as 20 mm. The mass unbalance in the rotor model is considered at the three rigid disks. The unbalance level of 440 gm-mm is assumed at each of the three disks. Similar unbalance is provided in the experimental rig also. The bearing coefficients, i.e. stiffness and damping, are assumed to be isotropic in the simulation model. The bearing stiffness is considered to be 1 MN/m as obtained from the experimental rig. The bearing stiffness is obtained from measured deflection of the shaft under known static load. The damping coefficient is taken 400 N-s/m as approximately calculated from the experimentally obtained unbalance response curve following half power point method. The equations of motion are solved using Runge-Kutta routine available in MATLAB for sufficiently long time to obtain steady state response at a particular rotor speed. The unbalance response curves are drawn using the magnitude of steady state response at various speeds from 500 to 29000 rpm. Unbalance response phase angle is also obtained from the simulation.

4. Experimental Rig

The effect of shaft bow on the unbalance response has been observed experimentally. The photograph of the rotor rig is shown in figure 2. The rotor rig consists of several mechanical components such as mild steel shaft, rigid disks, air turbine wheels, bearing supports. The rig was appropriately instrumented to acquire unbalance response at different locations and rotor speed using proximity probes. It was envisaged to cross the first critical speed during experimentation to observe the shaft bow effect. This necessitates higher damping in the bearing plane. Therefore, the ball bearings were mounted on elastomeric dampers to provide sufficient damping to cross the first critical speed. The rotor responses due to combined effect of shaft bow and unbalance at the middle disk and near the bearing location were measured. Experimental data were acquired using a high-speed data acquisition card through a personal computer. The data acquisition card has resolution of 14 bit and can take +/- 10 volt input signal. The shaft bow measured by slowly rotating the shaft for one complete revolution is shown in Fig. 3.

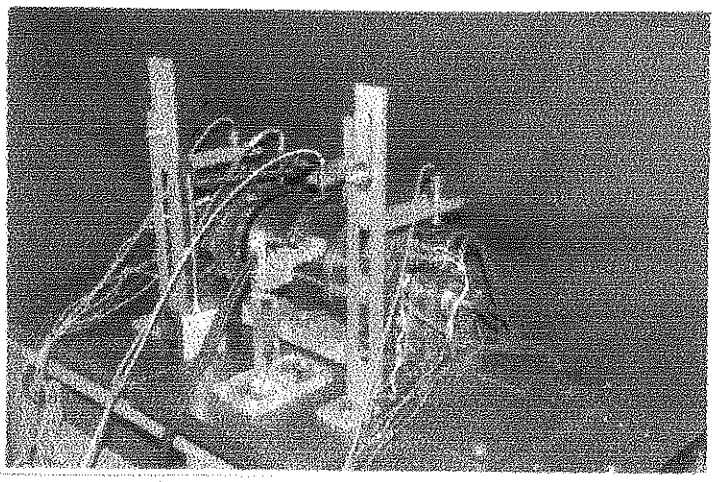

Fig. 2 Photograph of the experimental rig

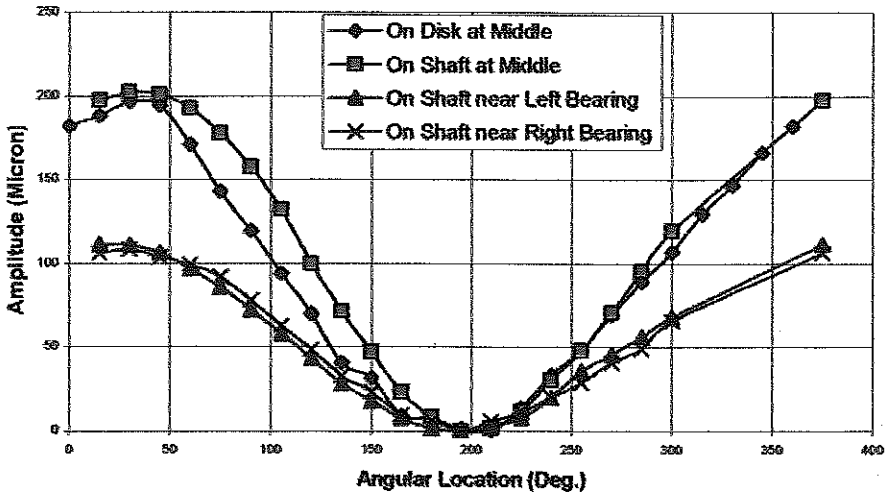

Fig. 3 Measured Shaft Bow

5. Results

The unbalance responses of a rotor-bearing system with initial shaft bow have been obtained by solving the equations of motion derived using finite element method. Simulated unbalance responses in vertical direction near the bearing location (approximately 50 mm away from the bearing) and at the middle disk is plotted for analysis purpose. Response results at other location are also available. Attempt has been made to validate the simulation results partly through experimentation. Fig. 4 shows the unbalance responses obtained with shaft bow near the bearing and at the middle disk locations. The initial shaft bow has little effect on the unbalance response at the middle disk for rotor speeds beyond the first critical speed. However, near the bearing location the response is increasing as the rotor speed is increased. Typical unbalance response characteristic of bent shaft is reflected in this figure as the response levels become very small at around 3000 rpm, which is close to the first critical speed of the rotor-bearing system. This phenomenon is well known from literatures and is called self-balancing. In case of multi mass rotor–bearing model one may not be able to consider a single bow factor parameter such as the ratio of bow magnitude and eccentricity in case of single mass rotor model. However, in the present case self-balancing has been observed at the first critical speed for the combination of bow vector and unbalance levels as mentioned in the previous section. Simulation has been carried out for higher bow effect by keeping the bow magnitude same, whereas the unbalance level is reduced by a factor of the square of the ratio of second and first critical speed. The unbalance response obtained from this simulation is shown in Fig. 5. It may be observed that the self-balancing is occurring near the second critical speed as expected.

In Fig. 6 and 7 unbalance responses near the bearing location and at the middle disk have been plotted, respectively, for three different cases, i.e. only unbalance, unbalance with bow at 180° phase with unbalance and unbalance with bow at 90° phase with unbalance. It may be observed from the figures that response level at the first critical speed is highest for the third case and lowest for the second case. However, response level in the second case is slightly higher than the other two cases for rotor speeds beyond second critical speed. The response phase angle is plotted in Fig. 8. The pattern of the variation of phase angle across the first critical speed in case of shaft bow is similar to previously published results.

The rotor responses due to the combined effect of initial shaft bow and unbalance at the middle disk and near the bearing location were measured. The measured responses are compared with the simulation results and shown in Fig. 9 and 10. It may be observed from figure 9 that the response at the middle disk reduces to a lower level just after the critical speed. It may be observed from Fig. 10 that the response near the bearing location is also reduced just after the critical speed but to a lesser extent than that at middle disk. There is good agreement between the experimental and the simulation results.

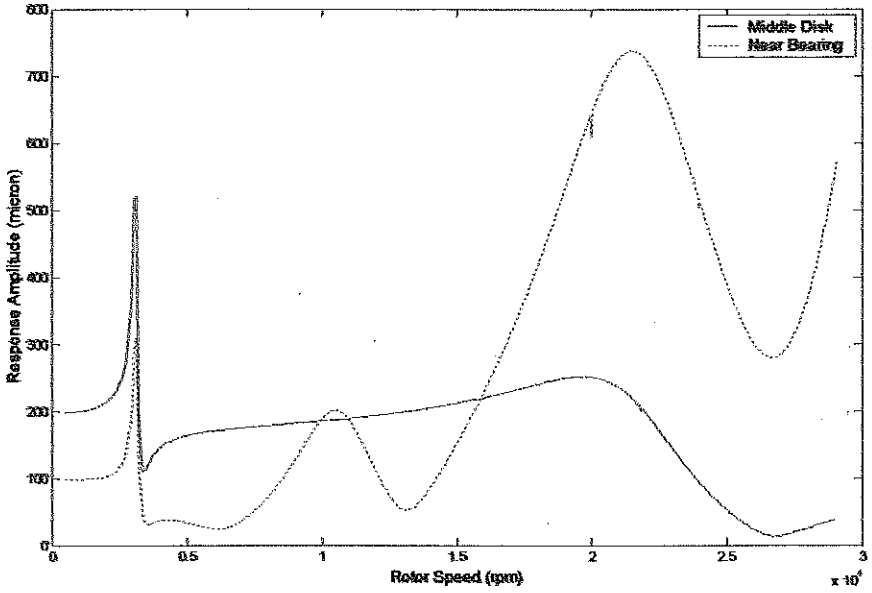

Fig. 4 Simulated unbalance response with initial shaft bow

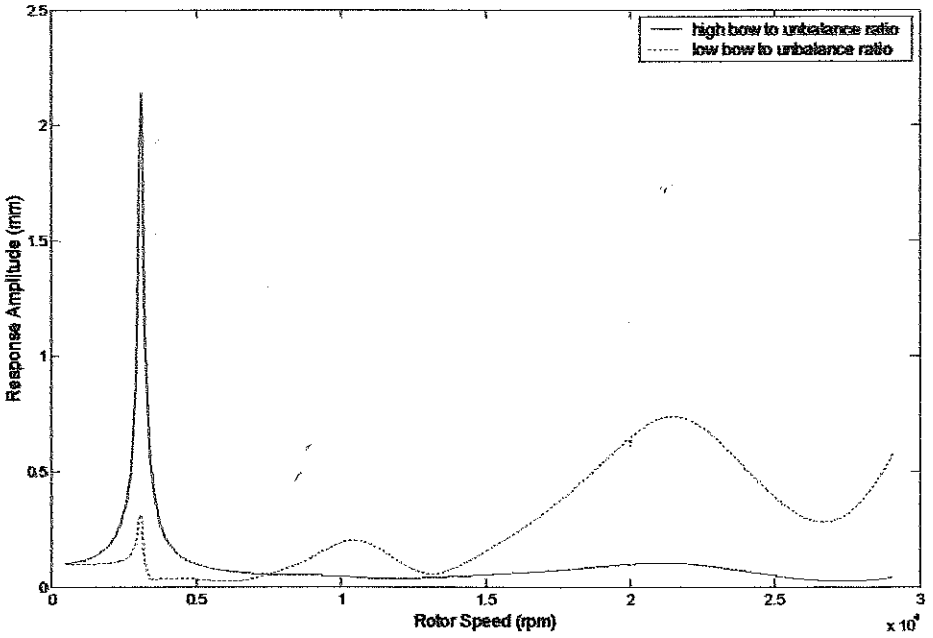

Fig. 5 Comparison of unbalance responses for different shaft bow to unbalance ratio

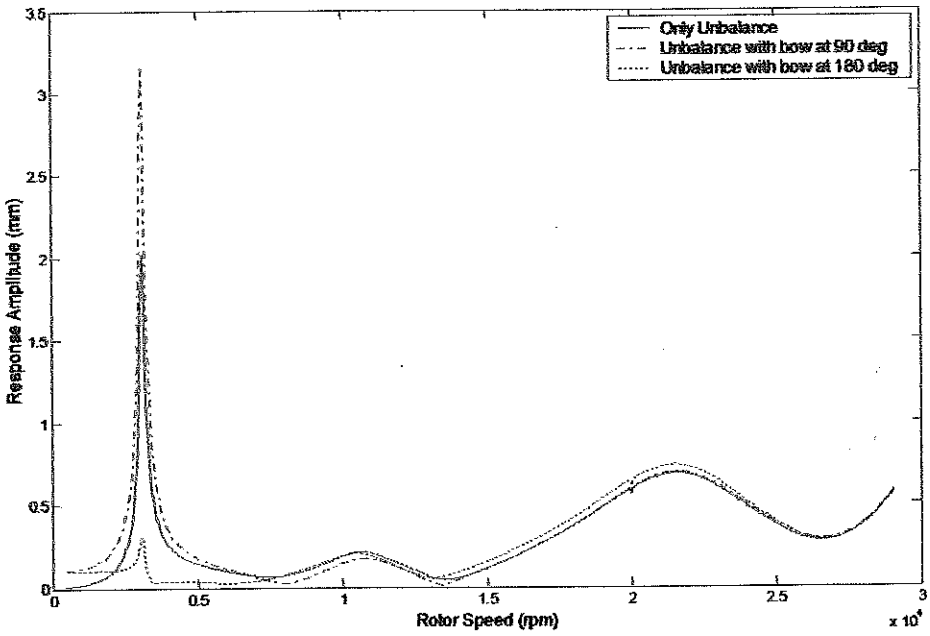

Fig.6 Comparison of unbalance response near bearing for bow at 90° and 180° phase with unbalance

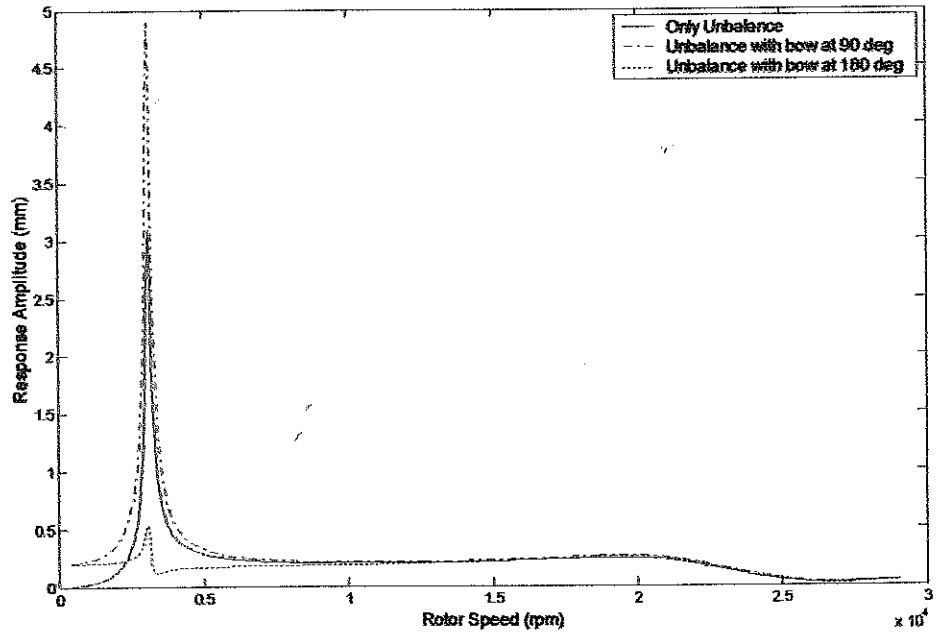

Fig.7 Comparison of unbalance response at middle disk for bow at 90° and 180° phase with unbalance

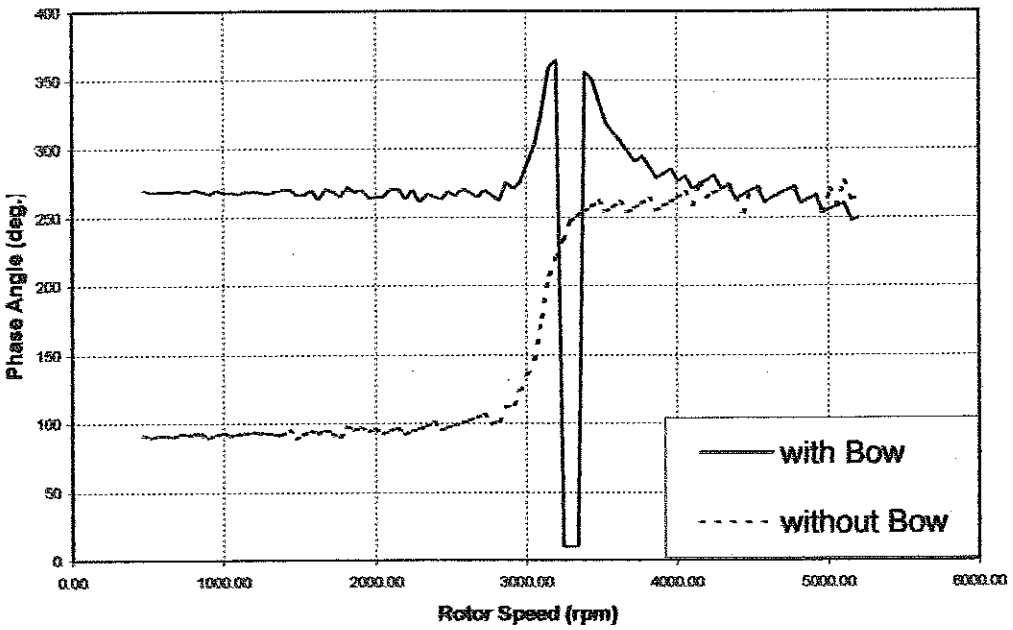

Fig. 8 Unbalance response phase relations

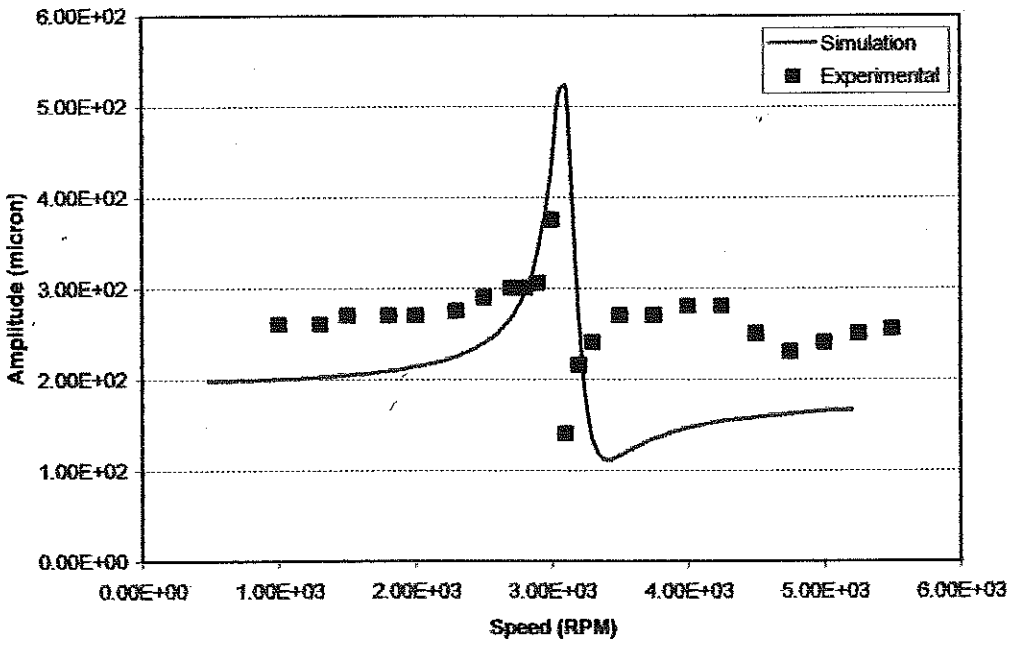

Fig 9. Comparison of simulated rotor response at the middle disk with measurement

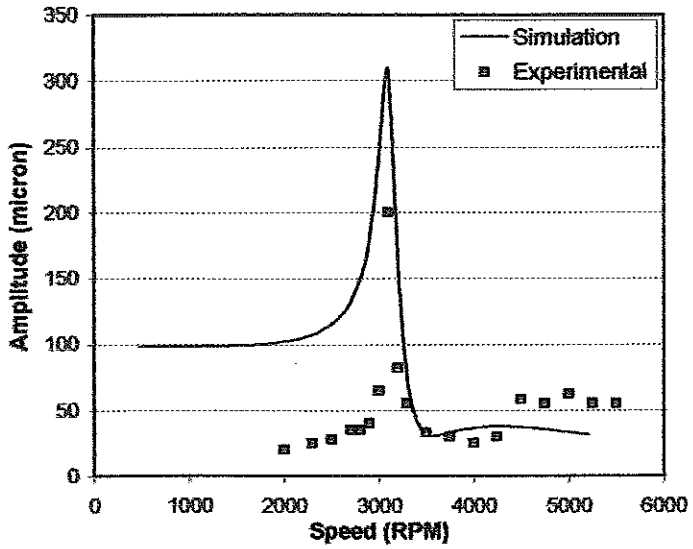

Fig. 10 Comparison of simulated rotor response near the bearing with measurement

6. Conclusions

An attempt has been made to predict the unbalance response of a rotor-bearing system with initial shaft bow using multi mass flexible rotor model. Finite element method has been adopted for the derivation of the equations of motion of the system. Simulations have been carried out for different cases of shaft bow magnitude and phase angle with respect to the unbalance. It has been observed that the shaft vibration level reduces to a very low value near the first critical speed for a particular bow magnitude and phase 180 deg apart from unbalance. This is called self-balancing, a typical characteristics, of bowed rotor. It is also observed through simulations that the occurrence of the self-balancing at a particular rotor speed depends on the relative magnitude of bow with the unbalance magnitude. The unbalance response beyond the first critical speed has also been obtained in the presence of shaft bow. Attempt has been made to validate the simulation results partly through experiments. There is good agreement between the simulation and experimental results.

Acknowledgements

The authors would like to acknowledge with thanks the help rendered by members of the Rotor Dynamics Group for their constant co-operation throughout the experimental investigation.

References

[1] J. C. Nicholas, E. J. Gunter and P. E. Allaire, *Effect of Residual Shaft Bow on Unbalance Response and Balancing of a Single Mass Flexible Rotor, Part I: Unbalance Response, Part II: Balancing*, Transactions of the ASME, Journal of Engineering for Power, Vol. 98, (1976), No. 2, pp 171-189.

[2] D. Salamone and E. J. Gunter, *Synchronous Unbalance Response of an Overhung Rotor with Disk Skew*, Journal of Engineering for Power, Vol. 102, (1980), pp 749-755.

[3] F. F. Ehrich, *Handbook of Rotordynamics*, McGraw Hill, 1992.

[4] J. S. Rao, *Vibratory Condition Monitoring*, Narosa, New Delhi, 2000.

[5] J. S. Rao and M. Sharma, *Dynamic Analysis of Bowed Rotors*, Proceedings of VETOMAC-1, October 25-27, (2000), IISc, Bangalore, India.

[6] A. G. Parkinson, M. S. Darlow and A. J. Smalley, *Balancing Flexible Rotating Shafts with Initial Bend*, AIAA Journal, Vol. 22, No. 5, (1984), pp 683-689.

[7] H. D. Nelson, *A Finite Rotating Shaft Element Using Timoshenko Beam Theory*, Transactions of the ASME, Journal of Mechanical Design, Vol. 102, (1980), pp 793-803.

[8] J. P. Den Hartog, *Strength of Materials*, 1st Edition, McGraw Hill Book Company, 1949.